Kinetically Controlled Selective Ionization Study on the Efficient Collisional Energy Transfer in the Deactivation of Highly Vibrationally Excited *trans*-Stilbene†

Heiko Frerichs, Matthias Hollerbach, Thomas Lenzer, and Klaus Luther*

Institut für Physikalische Chemie, Universität Göttingen, Tammannstrasse 6, D-37077 Göttingen, Germany

Received: August 15, 2005; In Final Form: December 1, 2005

Direct measurements of the gas-phase collisional energy transfer parameters are reported for the deactivation of highly vibrationally excited *trans*-stilbene molecules, initially prepared with an average energy of about 40 000 cm^{-1}, in the bath gases argon, CO_2, and *n*-heptane. The method of kinetically controlled selective ionization (KCSI) has been used. Complete experimental collisional transition probability density functions $P(E',E)$ are determined, which are represented by a monoexponential form with a parametric exponent in the argument, $P(E',E) \propto \exp[-\{(E - E')/(C_0 + C_1E)\}^{\gamma}]$ (for downward collisions), well established from earlier KCSI studies. A comparison of the first moments of energy transfer rate constants, $k_{E,1}$, or of resulting first moments of energy transfer, $\langle\Delta E(E)\rangle$, for *trans*-stilbene with those for azulene and toluene clearly shows the considerably more efficient deactivation of *trans*-stilbene for all bath gases, presumably due to the much greater number of very low-frequency modes of *trans*-stilbene. However, on a relative scale this gain in deactivation rate of excited *trans*-stilbene is clearly collider dependent and decreases distinctly with the growing collision efficiency of the larger bath gas molecules.

1. Introduction

Collisional energy transfer (CET) of highly vibrationally excited molecules is known to influence or even govern the rates and yields of many reactions.[1,2] Therefore it is important to get accurate information on the extent and details of this universal molecular process. For all moderate or larger size polyatomic molecules the situation at chemically relevant energies is characterized by very high densities of states such that even weak ubiquitous rovibrational state coupling results in an energetic quasicontinuum in which state to state energy transfer quantities lose their significance. Instead, continuous collisional transition probability density functions $P(E',E)$ are used to characterize the CET behavior. With the advent of the methods of kinetically controlled selective ionization (KCSI)[3] and more recently kinetically controlled selective fluorescence (KCSF)[4] it has become possible to obtain complete experimental sets of $P(E',E)$ distributions, as demonstrated in our studies on toluene and azulene deactivation.[4−6] This also includes at the same time the determination of very accurate values for the first moment of energy transfer, the average energy transferred per collision, $\langle\Delta E(E)\rangle$, as well as higher moments. Very recent theoretical attempts on the basis of modified statistical theories like PECT ("partially ergodic collision theory") have essentially confirmed the basic features of the $P(E',E)$ distributions found in the KCSI and KCSF studies and show great promise for the prediction of the CET transition probabilities for large molecular systems.[7−9]

In this contribution we present an investigation of *trans*-stilbene (*trans*-1,2-diphenylethylene) CET, which is so far the largest molecule studied by the KCSI technique. There have been no previous gas-phase CET investigations of this molecule, and this KCSI study together with ongoing very recent KCSF experiments[10,11] are the first to shed light on the behavior of this otherwise often studied molecule in isolated binary collisions. Comparison between energy transfer quantities of *trans*-stilbene, azulene and toluene can provide information on systematic trends concerning the CET behavior of polyatomic molecules.

2. Application of KCSI to *trans*-Stilbene

The principles of the KCSI method have already been described in full in our earlier publications,[3,5,6] so we focus here on the details of its application to the collisional relaxation of highly excited ground state *trans*-stilbene. A scheme of excitation and detection is depicted in Figure 1. As a precursor *cis*-stilbene is chosen and excited into the S_1 state by a 15 ns pump laser pulse at $\lambda_0 = 270$ nm ≙ 37 037 cm^{-1} (left side of Figure 1). This is followed by the very fast, nearly barrierless cis−trans isomerization reaction ($k_{c\rightarrow t} > 10^{12}$ s^{-1})[12] and a subsequent very fast internal conversion (IC) to the electronic ground-state S_0 ($k_{IC} > 10^{12}$ s^{-1}),[13,14] generating highly vibrationally excited *trans*- and *cis*-stilbene populations at a ratio of about 1:1. These are subsequently deactivated on a much longer time scale by collisions with a low-pressure bath gas M. After variable delay times Δt the S_0^* *trans*-stilbene molecules of a selected internal energy are detected by resonant 2-photon ionization via the S_1 intermediate state using a laser at wavelength λ_1 (shown on the right side of Figure 1). One-color ionization is feasible in this case, because the $S_0 \rightarrow S_1$ 0_0^0-transition (32 234.744 cm^{-1} ≙ 310.224 nm)[15] of *trans*-stilbene is located at an energy more than half of the adiabatic ionization potential (IP_t) of 61 748 cm^{-1}.[16] The ion yield of this resonant process strongly depends on the kinetic competition between up-pumping at λ_1 (k_{up}) and loss processes, where the total rate constant $k(E)$ is given by the sum of the trans−cis isomerization rate constant $k_{t\rightarrow c}$ (which is the dominant contribution above 1200 cm^{-1}) and the rate constant k_{rad} for radiative depopulation. Nonradiative processes are probably negligible.[17,18] This competition between ionization and the loss processes is governed by the energy dependence

† Part of the special issue "Jürgen Troe Festschrift".

10.1021/jp0545804 CCC: $33.50
Published on Web 01/11/2006

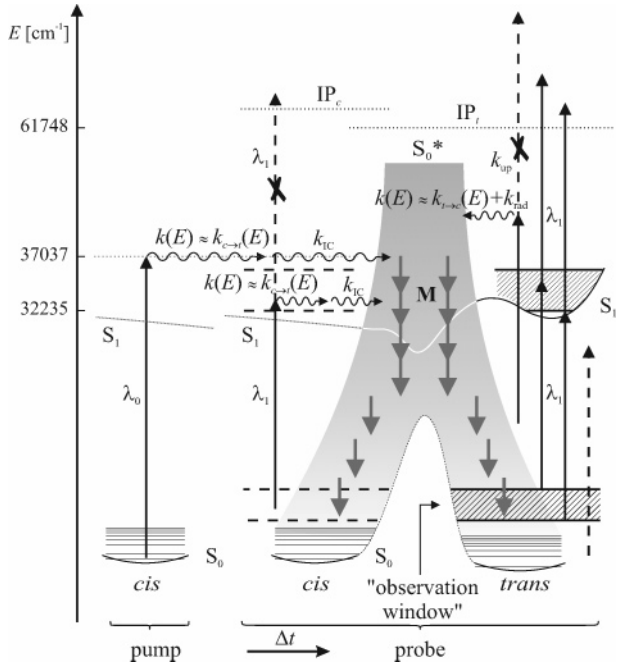

Figure 1. KCSI scheme for stilbene. Highly vibrationally excited *trans*-stilbene is generated by excitation of the cis isomer (λ_0, left side). After a time delay, the relaxing *trans*-stilbene molecules are detected by resonant 2-photon ionization (λ_1, right side). Kinetic competition in the intermediate state S_1 between the ionization step (rate constant k_{up} for up-pumping) and the cumulative rate constant $k(E)$ of *all* loss processes forms a so-called "observation window" for energy selective detection of vibrationally hot *trans*-stilbene molecules in the ground electronic state S_0. Note that on the trans-side the energy dependence of $k(E)$ is governed by the energy dependent trans−cis isomerization reaction rate constant $k_{t\rightarrow c}(E)$. Below the barrier only fluorescence is important, and nonradiative processes can be neglected. For further details see the text.

of the isomerization reaction (see below). Note that the present study uses for the first time an energy dependent reaction rate—instead of a radiationless transition—as kinetic competition to specify the energetic shape of the KCSI observation window.

In a simplified scheme, the potential energy surface of the cis−trans isomerization in S_1 can be sketched by assigning the torsional angle around the ethylenic double bond to the reaction coordinate (right side of Figure 1). Starting from the trans side, the stilbene molecule has to overcome a barrier of about 1150 cm^{-1} to react and reach the configuration at an angle of 90° (often called the "phantom state" in the literature), from which a very fast IC to S_0 occurs.[13,14,18,19] Due to the strong increase of the isomerization rate constant $k_{t\rightarrow c}(E)$ with excess energy the effective ionization is limited to the relatively narrow region from the origin up to energies not far above the barrier. By the choice of wavelength λ_1 this energy regime for ionization is projected down onto the energy scale of the ground electronic state defining a "detection window" of vibrational energy for selective observation of the relaxing population. The lower edge of this "observation window" is defined by the minimum vibrational energy necessary to reach S_1 with a photon λ_1 whereas its upper limit is determined by the competition between $k_{t\rightarrow c}(E)$ and the pumping rate for the ionization step. By tuning λ_1, one can shift the observation window on the S_0 energy scale. The collisional deactivation of the simultaneously generated cis isomer does not interfere as it cannot be ionized at our laser intensities due to its very short lifetime in the intermediate S_1 state. This is also supported by our KCSI measurements, because essentially no ions are produced even under the much more favorable conditions of the pump pulse at λ_0. The cis and trans isomers in S_0 relax independently of each other in their respective potential wells due to the high isomerization barrier of 17 000 cm^{-1}.[20] We have confirmed this by simplified master equation simulations (not shown here) using RRKM estimates for the isomerization rate constants assuming reasonable frequencies for the reactands and the transition state. These show that isomerization in S_0 is far too slow to play any role on the microsecond time scale of the KCSI experiments at the pressures used.

TABLE 1: Lennard-Jones Collision Numbers and Potential Parameters for Collisions between *trans*-Stilbene and a Bath Gas M

bath gas	σ_M (Å)	ϵ_M/k_B (K)	T (K)	$10^{-7}Z_{LJ}$ ($mbar^{-1}$ s^{-1})	$10^{10}Z_{LJ}$ (cm^3 s^{-1})
trans-stilbene	7.72	524.5			
Ar	3.47	113.5	305	1.479	6.234
CO_2	3.94	201	303	1.793	7.512
n-heptane	6.65	351	304	2.331	9.799

3. Observation Window Functions and KCSI Simulations for *trans*-Stilbene

In a KCSI experiment the ion yield is recorded as a function of the pump−probe delay time, resulting in a transient ion signal, which reflects the passage of the relaxing population through the corresponding energetic observation window. Lennard-Jones collision numbers (Z_{LJ}) are used to convert the time scale into a reduced "number-of-collisions" axis (see Table 1 for a summary of the systems studied here). The arrival time of the signal and in particular its shape, which is directly related to the shape of the relaxing distribution, include all important information about the collisional transition probability $P(E',E)$. The KCSI ion signal at a specific time is represented by[4]

$$I_D(t) \propto \int_0^\infty g(E,t)\, W_{KCSI}(E,\lambda_1)\, dE \qquad (1)$$

where $W_{KCSI}(E,\lambda_1)$ is the energy dependent ionization probability for the probe wavelength λ_1 describing the observation window ("window function"), and $g(E,t)$ is the time dependent population g at time t and energy E.

For a 2-photon ionization process, as described above, with not too high optical pumping, mostly realized with nanosecond laser pulses, the relation between the ion yield and the excess energy dependent rate constant $k(E)$ of the loss processes is given by the expression[6]

$$W_{KCSI}(E(S_0^*),\lambda_1) \propto \epsilon_1(\lambda_1,E(S_0^*))\,\epsilon_2(\lambda_1,E(S_1^*))[1 + (k(E(S_1^*))\tau_{eff})^{4/3}]^{-3/4} \qquad \text{for } E \geq E_{low} \quad (2)$$

E_{low} is the minimum energy in S_0 at which resonant 2-photon ionization becomes possible, i.e., $E_{low} = E_{0-0}(S_1) - hc/\lambda_1$, where $E_{0-0}(S_1)$ is the 0_0^0 $S_0 \rightarrow S_1$ transition energy of *trans*-stilbene. ϵ_1 and ϵ_2 are the wavelength and energy dependent absorption coefficients in the S_0 and S_1 states, respectively. τ_{eff} is the effective laser pulse width.[4] A variety of $k(E)$ data obtained from lifetime measurements in molecular beam experiments as well as thermal samples are available from several sources.[21−30] An overview is given in Figure 2. Note that $k(E)$ contains the sum of all possible processes leading to depletion of the S_1 state population (mainly isomerization and fluorescence). The energy dependence is completely governed by the rate constant of the trans−cis isomerization. There is some scatter in the $k(E)$ data

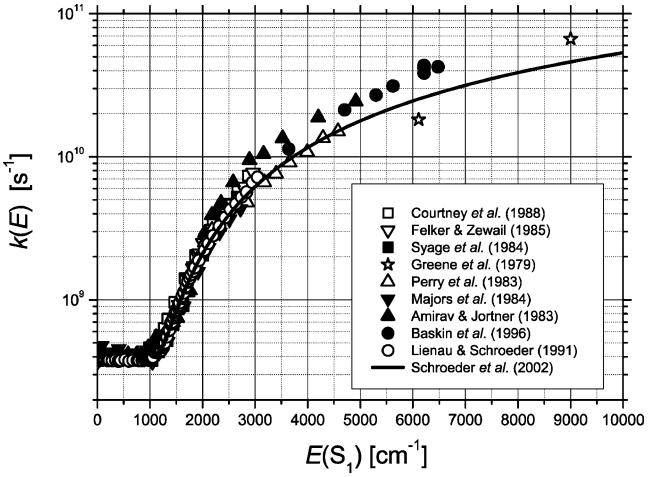

Figure 2. $k(E)$ data for the *trans*-*cis* isomerization of stilbene in the S_1 state. Points are time-resolved measurements from different groups.[21−30] The solid line corresponds to the RRKM expression given by Schroeder et al.[19]

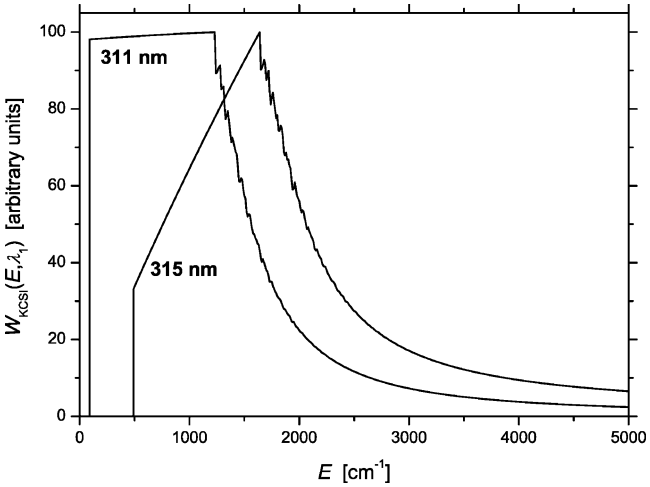

Figure 3. Normalized KCSI observation windows for *trans*-stilbene at the probe wavelengths $\lambda_1 = 311$ and 315 nm.

especially for energies above 3000 cm^{-1}. The points can be reasonably fitted by the RRKM expression given by Schroeder et al., shown as a solid line.[19] Although the applicability of a RRKM approach in the specific case of the excited-state trans−cis isomerization of stilbene is still under debate,[31] we use the expression of Schroeder et al. as a successful empirical description of the available experimental data.

For the calculation of the window functions the energy dependent absorption coefficients for the two absorption steps $S_0 \rightarrow S_1$ (ϵ_1) and $S_1 \rightarrow I^+$ (ϵ_2) are also required. There is strong experimental indication that ϵ_2 is practically energy independent in the regime of interest.[6] For the probe wavelengths 311 and 315 nm, values for $\epsilon_1(\lambda_1,E)$ are available from "hot" UV absorption spectra, $\epsilon_1(\lambda_1,T)$, recorded in a heatable cell by Schwarzer and co-workers. The energy dependence at the two wavelengths can be well approximated by their empirical expressions:[10]

$$\epsilon_1(311\text{ nm},E) = (E + 10050)^{0.95} \cdot 2.490 \times 10^{-5} \times \exp[-0.72 \times 10^{-4}(E + 10050)] \quad (3)$$

$$\epsilon_1(315\text{ nm},E) = E^{0.99} \cdot 1.095 \times 10^{-5} \times \exp[-0.80 \times 10^{-4}E] \quad (4)$$

In the current analysis of a still relatively small data set we use the window functions W_{KCSI} as calculated from external photophysical parameters by eq 2 for simulation of the KCSI results. Note that in our KCSI study on azulene we could demonstrate excellent agreement between such calculated window functions and those obtained via "self-calibrating" measurements (i.e., sets of varied measurements which even provide unique extraction of the window functions directly from KCSI data by the master equation analysis without need to use any photophysical parameters as input).[6] With the reported set of pump and probe wavelengths, determined by some technical constraints, such "self-calibration" in this system cannot be achieved. However, at present we are extending our measurements to record KCSI signals of *trans*-stilbene relaxation at additional sets of pump and probe wavelengths, with the goal to fully achieve the quality of "self-calibrated" results.

The resulting normalized window functions for *trans*-stilbene are shown in Figure 3. With increasing wavelength the windows are shifted toward higher energies. The zigzag shape on the early falling edge of each window stems from the RRKM fit and is caused by the discrete structure of the transition state's sum of states at low excess energies in S_1. The steepness of the falling edge is determined by the competition between $\epsilon_1(\lambda_1,E)$, which increases with ground-state vibrational energy, and the decreasing lifetime of the intermediate state S_1 (Figure 2). For the slow decrease at high energies above 9000 cm^{-1} only calculations are available. However, preliminary KCSI data for the probe wavelength 320 nm show that the window amplitude above this energy must be negligible. Therefore in this work the windows are cut off at 10 000 cm^{-1}, i.e., $W_{KCSI}(E,\lambda_1)$ is set to zero above this energy probably without adding much uncertainty at the present level. The problem will be analyzed in more detail in a future publication.

Having established the shape of the windows, a forward fitting procedure using a master equation approach is carried out simultaneously for all windows to extract $P(E',E)$ for a specific bath gas from the KCSI signals at different wavelengths, as described in detail before.[5] As in our earlier studies, we employ for the transition probability our flexible exponential functional form with a parametric exponent Y in the argument, which has been used very successfully to evaluate consistently all KCSI curves of toluene and azulene CET in wide varieties of bath gases:[5,6]

$$P(E',E) = \frac{1}{c(E)} \exp\left[-\left(\frac{E - E'}{C_0 + C_1E}\right)^Y\right] \qquad \text{with } E' \le E \quad (5)$$

Here $c(E)$ is a normalization factor, and three parameters, C_0, C_1, and Y, are varied to obtain the best fit to the experimental data. The upper wing of the transition probability ($E' > E$) is determined by detailed balance. For this the thermal Boltzmann distribution $f(E)$ has to be calculated. We used a Beyer−Swinehart direct count algorithm[32] employing the following 72 experimental vibrational frequencies $\tilde{\nu}_i = \nu_i/c$ (in cm^{-1}) for *trans*-stilbene obtained by Schroeder and co-workers on the basis of B3LYP/6-311+G(d) calculations: 3068, 3067, 3060, 3060, 3051, 3050, 3041, 3041, 3034, 3034, 3024, 3015, 1625, 1583, 1575, 1557, 1552, 1477, 1470, 1432, 1423, 1327, 1321, 1308, 1304, 1280, 1242, 1208, 1166, 1164, 1162, 1140, 1140, 1064, 1062, 1011, 1009, 977, 976, 961, 953, 945, 930, 929, 900, 881, 849, 846, 810, 809, 802, 748, 719, 672, 670, 631, 613, 609, 531, 524, 458, 455, 397, 393, 280, 276, 216, 197, 84, 75, 57, 11.[33]

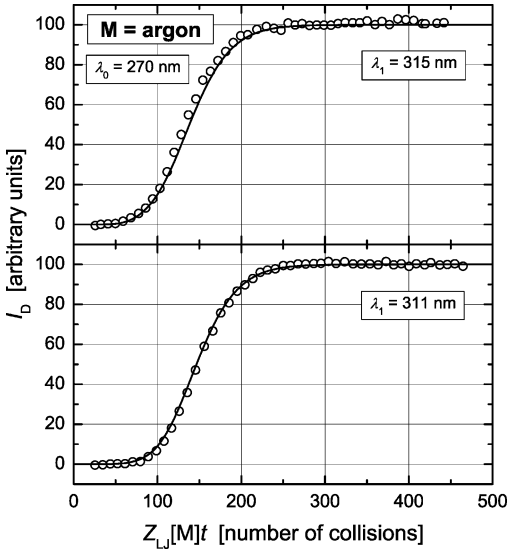

Figure 4. KCSI data for the deactivation of *trans*-stilbene by argon. The lines represent the best fit obtained from a master equation analysis using the $P(E',E)$ form given by eq 5 with the parameters listed in Table 2.

Starting with the initially produced *trans*-stilbene distribution, integration of the master equation

$$\frac{dg(E,t)}{d(Z[M]t)} = \int_0^\infty [P(E,E')\, g(E',t) - P(E',E)\, g(E,t)]\, dE' \qquad (6)$$

provides the time evolution of the population $g(E,t)$.[5] The simulated KCSI signals obtained from convolution of this $g(E,t)$ with the window functions $W(E,\lambda_1)$ (eqs 2−4) are compared with the normalized experimental curves.

4. Experimental Section

The KCSI experimental setup and the ionization cell have been already described in detail in earlier publications.[3,5,6] Therefore only a brief overview is given here. The pump wavelength $\lambda_0 = 270$ nm (pulse energy 10−20 μJ, duration 15 ns, beam diameter 1.4 mm) and the probe wavelengths $\lambda_1 =$ 311 or 315 nm (350−600 μJ, 2.5 mm) were generated by two excimer-pumped dye lasers, using coumarine 153 and rhodamine 101, with subsequent frequency-doubling in BBO crystals. Ions were detected by a sensitive capacitor arrangement as described earlier.[3] All measurements were performed in a steady-state flow system with pressures of 11−30 mbar for argon, 4−13 mbar for CO_2 and 1 mbar for *n*-heptane. The *cis*-stilbene sample (Lancaster, 97%) was used without further purification and kept in the dark at room temperature (25−30 °C). Argon and CO_2 were fed via a flow controller from a high-pressure gas cylinder into the ionization cell. Liquid *n*-heptane (Merck, Uvasol) was kept at 0 °C and its vapor was fed into the cell via a needle valve. The cell windows were heated to 50 °C to avoid deposition of stilbene.

5. Results and Discussion

The normalized KCSI curves resulting from the deactivation of *trans*-stilbene by the collider gases argon, CO_2 and *n*-heptane, respectively, are shown in Figures 4−6. They were obtained by averaging 9−13 measurements. The corresponding Lennard-Jones parameters and collision numbers used to reduce the time

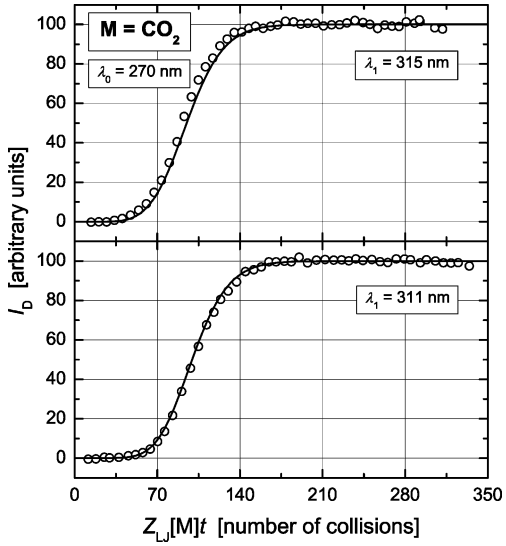

Figure 5. Same as in Figure 4, but for the bath gas CO_2.

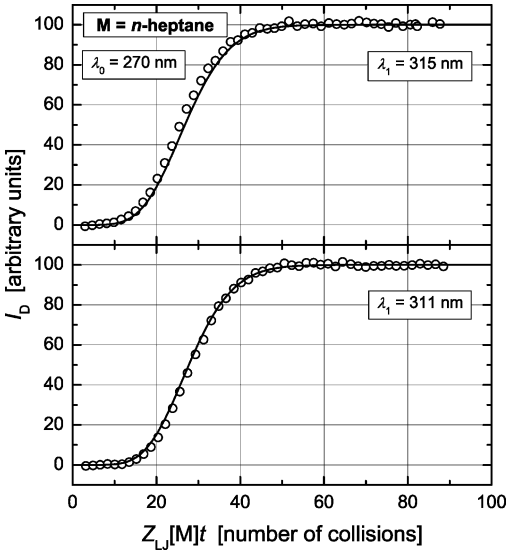

Figure 6. Same as in Figure 4, but for the collider *n*-heptane.

axis to a number of collisions scale are listed in Table 1.[3] In the case of *trans*-stilbene, Lennard-Jones parameters were estimated using the method of Tee, Gotoh and Stewart via its critical temperature, critical pressure, and boiling point (580 K).[34−36] Critical data were estimated using atom, structure and group increments (two benzene rings, two tertiary C atoms and one nonaromatic C=C double bond), as described by Ambrose.[37]

In contrast to our earlier KCSI studies on azulene and toluene,[5,6] the residual ion signals of *trans*-stilbene at long time delays, which represent the fraction of the completely relaxed distribution extending into the respective observation window, always reach the highest relative level of 100% and no KCSI curves with maxima have been recorded so far. This is due to the fact that the thermal distribution of *trans*-stilbene resides at a much higher average energy than for the other systems studied before.

A characteristic point for a first visual inspection of the KCSI curves is the number of collisions at half-maximum ("$Z_{1/2}$" = $Z_{LJ}[M]t_{1/2}$). For 315 nm it is about 10% smaller than at 311 nm for all three colliders. This difference approximately reflects the average number of collisions necessary to decrease the energy of the relaxing *trans*-stilbene population by the difference

TABLE 2: Parameters for the Monoexponential Transition Probability $P(E',E)$ with Parametric Exponent Y and Energy Dependent Parameter $\alpha(E) = C_0 + C_1E$ (See Eq 5), As Obtained from Master Equation Simulations

bath gas	C_0 (cm^{-1})	C_1 (10^{-3})	Y
Ar	87	9.57	0.7
CO_2	240	16.6	0.9
n-heptane	1100	74.2	1.5

of energies between the observation windows. As expected, these values for the different colliders (argon > CO_2 > *n*-heptane) illustrate the increase of deactivation efficiency when the bath molecules are ordered by their number of degrees of freedom.

The solid lines in Figures 4−6 represent our current best master equation fits to the experimental curves. For each bath gas the fits were made simultaneously to the 315 and 311 nm curves. The corresponding $P(E',E)$ parameters are given in Table 2. They show the same systematic properties as found in the earlier systems studied by KCSI. The values of C_0 and C_1, characterizing the energy dependent exponential denominator $\alpha(E) = C_0 + C_1E$ (see eq 5), increase strongly in the order Ar, CO_2, *n*-heptane, as observed also with toluene and azulene. Moreover, the data confirm a systematic variation in the exponential shape of $P(E',E)$, given by the parameter Y of eq 5, dependent on the size of the bath gas collider: Small colliders (Ar, CO_2) show Y values <1, i.e., "extended" exponential tails of $P(E',E)$ ("concave" in a semilogarithmic plot), whereas a "reduced" exponential tail (semilogarithmically "convex" shaped) with $Y = 1.5$ is found for the large collider *n*-heptane.

This bath gas dependent variation of the $P(E',E)$ functional shape has been found experimentally for the first time by the KCSI measurements of toluene and azulene energy transfer.[5,6] Very interestingly the Y dependence on the colliders could recently be well reproduced by a single parameter, purely statistical PECT-model, without reference to dynamical features.[7−9]

Inspection of Figures 4−6 shows that there is a systematic mismatch of the fits, as can be seen from the difference at $Z_{1/2}$ between the signals for 311 and 315 nm, which is slightly smaller in the simulations than in the experiments for all three colliders. This might be due to some still unidentified imperfection in the shape of the calculated windows. It is not possible to remove this deviation by changing the $P(E',E)$ parameters. Accordingly, the present values of the $P(E',E)$ parameters for *trans*-stilbene are probably less well determined than for the other systems in the earlier KCSI studies. In addition, the conditions for measurements are somewhat less favorable, if, e.g., absorption coefficients give access mainly to observation windows at low energies as in the case of *trans*-stilbene. Experimental signals of simple monotonic shape like in Figures 4−6 contain much less information than those from observation windows at higher energies in which relaxation results in KCSI signals of mathematically more complex shapes including various pronounced maxima, as observed, e.g., in toluene and azulene.[5,6] For instance, a residual ion signal of less than 100% imposes severe constraints on the shapes of the observation windows and the values of the $P(E',E)$ parameters, because the master equation simulations are very sensitive to these parameters. Further measurements are thus underway to probe at longer wavelengths (i.e., higher energy observation windows) for types of signals that pose more severe restrictions on the best fit parameters of the master equation simulations. In addition, currently performed studies at significantly shorter pump wavelengths shall support further improved precision in $P(E',E)$.

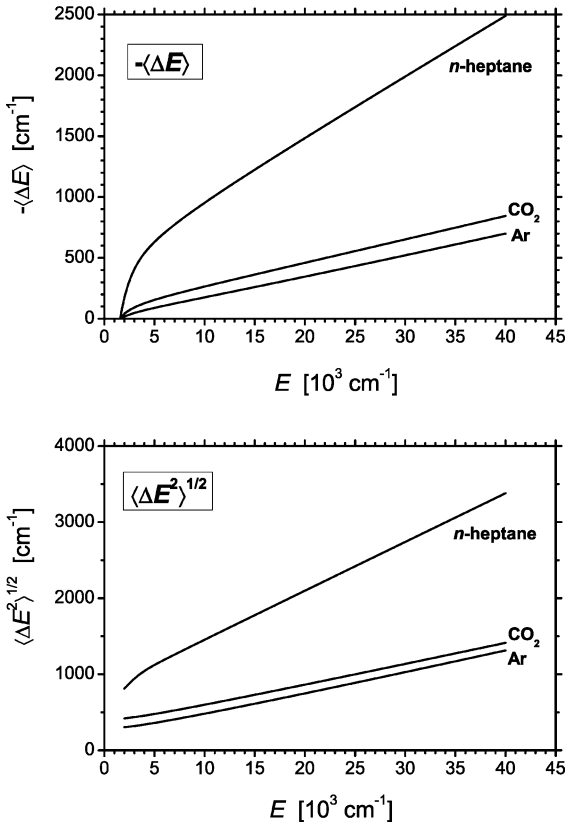

Figure 7. First moment of energy transfer, $\langle\Delta E\rangle$, and square root of the second moment of energy transfer, $\langle\Delta E^2\rangle^{1/2}$, as a function of energy for the deactivation of *trans*-stilbene by the colliders argon, CO_2, and *n*-heptane. See also Tables 3−5.

TABLE 3: $\langle\Delta E\rangle$ Values Calculated from Optimized $P(E',E)$ (Parameters in Table 2)

	$-\langle\Delta E\rangle$ (cm^{-1})			
bath gas	10 000 cm^{-1}	20 000 cm^{-1}	30 000 cm^{-1}	40 000 cm^{-1}
Ar	176	346	521	700
CO_2	264	460	652	845
n-heptane	953	1484	1990	2489

TABLE 4: $\langle\Delta E^2\rangle^{1/2}$ Calculated from Optimized $P(E',E)$ (Parameters in Table 2)

	$\langle\Delta E^2\rangle^{1/2}$ (cm^{-1})			
bath gas	10 000 cm^{-1}	20 000 cm^{-1}	30 000 cm^{-1}	40 000 cm^{-1}
Ar	481	748	1028	1313
CO_2	599	863	1136	1413
n-heptane	1454	2098	2739	3380

The resulting energy dependent first and second moments of energy transfer, i.e., the average energy transferred per collision and the root-mean-squared energy transferred per collision, $\langle\Delta E(E)\rangle$ and $\langle\Delta E(E)^2\rangle^{1/2}$, are listed for selected energies in Tables 3 and 4 and displayed in Figure 7. Parameters for corresponding fitting polynomials are given in Table 5. It is important to note that the overall uncertainties in $\langle\Delta E(E)\rangle$ from KCSI are much smaller than in single parameters of $P(E',E)$. This can be rationalized by considering that $\langle\Delta E(E)\rangle$ is mainly sensitive to the arrival times of the KCSI signals. We thus estimate that the current error in $\langle\Delta E(E)\rangle$ is not more than ±10%, only slightly worse than in the systems studied earlier.[5,6]

Comparison of the $\langle\Delta E(E)\rangle$ values in Table 3 with corresponding earlier results for toluene and azulene shows that the energy transfer of *trans*-stilbene is much more efficient with each of the colliders. The energy transfer property of prime

TABLE 5: Third-Order Polynomial Fits to the First and Second Moments of Energy Transfer for Collisions between *trans*-Stilbene and the Collider M[a]

	$\langle\Delta E\rangle$				$\langle\Delta E^2\rangle^{1/2}$			
bath gas	A_0 (cm^{-1})	10^3A_1	10^8A_2 (cm)	$10^{13}A_3$ (cm^2)	A_0 (cm^{-1})	10^3A_1	10^8A_2 (cm)	$10^{13}A_3$ (cm^2)
Ar	−7.26	−16.66	−1.12	−1.36	240.80	22.58	17.27	−16.87
CO_2	−50.25	−22.39	12.65	−16.01	355.89	23.20	13.54	−13.83
n-heptane	−325.90	−67.70	62.66	−72.33	797.10	66.28	−7.79	8.88

[a] Valid from 5000 to 40 000 cm^{-1}. $\langle\Delta E\rangle = A_0 + A_1E + A_2E^2 + A_3E^3$ and $\langle\Delta E^2\rangle^{1/2} = A_0 + A_1E + A_2E^2 + A_3E^3$ Calculated using the $P(E',E)$ of eq 5 with the parameters from Table 2.

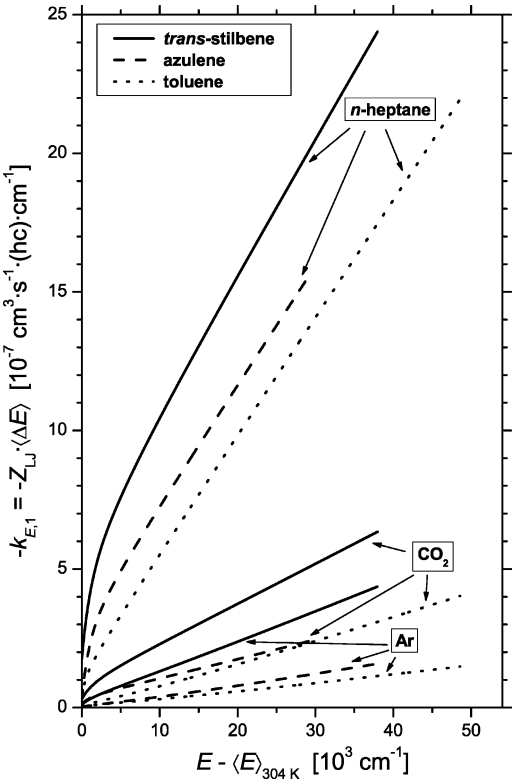

Figure 8. First moment $k_{E,1}$ of the energy transfer rate coefficient $k(E',E)$ for collisions between *trans*-stilbene and several bath gases (solid lines) in comparison with the corresponding quantities for the collisional deactivation of azulene (dashed lines) and toluene (dotted lines), respectively.

importance for chemistry in molecular ensembles is the rate of deactivation (or activation) determining, e.g., the overall reaction rate or the extent of energy transfer induced branching in reactive systems. We thus use energy transfer rates instead of $\langle\Delta E(E)\rangle$ values to compare the efficiencies of different systems. This includes the effect of variations in the collision numbers and avoids the unsolved problem of their possible energy dependence. In Figure 8, $k_{E,1}$, the first moment of the energy transfer rate constant $k(E',E)$, defined as

$$k_{E,1} = Z_{LJ}\langle\Delta E(E)\rangle \quad (7)$$

is plotted against the excess energy above room temperature (304 K) average energy, $E - \langle E\rangle_{304K}$, for *trans*-stilbene, azulene, and toluene with Ar, CO_2, and *n*-heptane, respectively, as colliders. The much faster deactivation of *trans*-stilbene versus azulene or toluene in all bath gases is clearly shown, with only a smaller contribution due to variations in the number of molecule-bath gas collisions per unit time. The increase of $\langle\Delta E(E)\rangle$ with size or complexity of the energy donor does not come unexpected. For explaining large $\langle\Delta E(E)\rangle$ from *trans*-stilbene it appears of course reasonable to refer to the large number of low-frequency vibrations (4 modes with <100 cm^{-1}, 12 with <500 cm^{-1}) and the large flexibility of the molecular frame compared with, e.g., the relatively stiff azulene with only one mode of <200 cm^{-1} (7 with <500 cm^{-1}). Such a trend is expected already from simple approaches such as Landau−Teller type models and also found in classical trajectory studies.[38−41] However, closer comparison of the increase of $\langle\Delta E(E)\rangle$ from toluene to *trans*-stilbene in the three bath gases reveals apparent tendencies which are not easily rationalized and raise various open questions. The data in Figure 8 indicate that the relative change of the relaxation efficiency in the toluene/azulene/*trans*-stilbene series decreases with increasing collider size and efficiency, i.e., in the order Ar > CO_2 > *n*-heptane. Table 6 gives the ratios of $k_{E,1}$ between *trans*-stilbene and azulene or toluene, respectively, in the three bath gases at selected energies. As a typical example the ratios of $k_{E,1}$ between stilbene and azulene at 20 000 cm^{-1} decrease from 3.0 to 2.1 and 1.3 for Ar, CO_2 and *n*-heptane, respectively, and the same trend is found in the comparison with toluene. This might point toward some sort of "saturation effect" in collisional efficiency for increasing size of the collider at the deactivation of large enough molecules. Such interpretation will of course need further confirmation by additional KCSI or KCSF measurements for other bath gases.

TABLE 6: Ratio between $k_{E,1}$ of *trans*-Stilbene and Azulene or Toluene, Respectively, in Several Bath Gases at Selected Energies

		$k_{E,1}$(*trans*−stilbene)/$k_{E,1}$(molecule A)		
molecule A	$E - \langle E\rangle_{304K}$ (cm^{-1})	Ar	CO_2	*n*-heptane
azulene	10 000	3.3	2.2	1.4
	20 000	3.0	2.1	1.3
	30 000	2.8	2.1	1.3
toluene	10 000	4.3	3.0	1.9
	20 000	4.1	2.4	1.6
	30 000	3.9	2.2	1.5

The results of this work represent a marked deviation from the usual expectation of similarly enhanced deactivation rates for all bath gases in the case of a large molecule like *trans*-stilbene compared with, e.g., azulene, due to the much larger number of CET-active vibrational modes in *trans*-stilbene. Of course there is a principal upper limit to CET efficiency. However, the observed trend of saturation behavior does not simply correspond to an approach of the ergodic statistical limit of CET. Relations between both have to be clarified. The strong influence of collider size on the saturation tendency is even emphasized by looking at the sizes of the absolute increments, $\Delta k_{E,1}$, between our various energy donors in a given bath gas (e.g., at 20 000 cm^{-1} internal energy). From toluene to azulene these $\Delta k_{E,1}$ increments are quite similar in Ar and CO_2 as bath gases, but about 10 times bigger in *n*-heptane. From azulene to *trans*-stilbene the $\Delta k_{E,1}$ increments in Ar and CO_2 are again close to each other, but now the increase for *n*-heptane as a bath gas is merely by a factor of 2. Remarkably, the $\Delta k_{E,1}$

increments between the three donor systems of Figure 8 in *n*-heptane show scarcely an energy dependence over a very wide range of excitation. Explanations of the collider dependences of the saturation trends also have to include the consequences for reversal of the role of donor and acceptor and the singular case of identical donors and acceptors in self-quenching. Evidently, the details of dynamic properties of CET have to be analyzed, e.g., via trajectory calculations to reach a valid understanding.

Clearly, the influence of intramolecular vibrational redistribution (IVR) as a possible dynamical bottleneck has to be considered. One could, e.g., think of a limited energy flow in the *trans*-stilbene molecule. In a very simple picture, a larger collider could then, e.g., remove only the excess energy in that part of the molecule, where the closest interaction occurs, whereas after removal there is not enough time for the rest of the excess energy to redistribute throughout the *trans*-stilbene molecule on the time scale of the collision. The main handicap for validation of answers on the above and further related questions is the fact that we do not yet have sufficiently broad bases of corresponding experimental CET data of an equally high level of validity. The present work is thought as a step in supplying such basis for fully comparable high quality data in the regime of large molecule energy transfer.

6. Conclusions

The CET of highly vibrationally excited *trans*-stilbene has been studied for the first time in the gas phase. Our KCSI eperiments clearly show that *trans*-stilbene is much more efficiently deactivated than azulene or toluene, which both have been studied previously by KCSI and KCSF methods. This is most likely due to the larger number of modes with very low frequencies. The change of the extracted preliminary $P(E',E)$ parameters with collider size is also consistent with our earlier studies. We plan to extend our investigations to larger probe wavelengths (i.e., higher lying detection windows), shorter pump wavelengths (to cover a wider energy range) and a wider set of colliders, to further study the interesting CET properties of this efficient molecule.

Acknowledgment. We thank Jürgen Troe, Jörg Schroeder, Dirk Schwarzer, Christian Reichardt and Kawon Oum for very helpful discussions, and Reinhard Bürsing for his excellent technical assistance. This work has been financially supported by the Deutsche Forschungsgemeinschaft [SFB 357 ("Molekulare Mechanismen unimolekularer Prozesse", A7)]. It is also a pleasure to acknowledge the close cooperation with Sture Nordholm and Daniel Nilsson (University of Göteborg) on all theoretical aspects of the current work.

References and Notes

(1) Hippler, H.; Troe, J. In *Bimolecular Collisions*; Baggott, J. E., Ashfold, M. N. R., Eds.; The Royal Society of Chemistry: London, 1989; p 209.

(2) Oref, I.; Tardy, D. C. *Chem. Rev.* **1990**, *90*, 1407.

(3) Hold, U.; Lenzer, T.; Luther, K.; Reihs, K.; Symonds, A. C. *J. Chem. Phys.* **2000**, *112*, 4076.

(4) Frerichs, H.; Lenzer, T.; Luther, K.; Schwarzer, D. *Phys. Chem. Chem. Phys.* **2005**, *7*, 620.

(5) Lenzer, T.; Luther, K.; Reihs, K.; Symonds, A. C. *J. Chem. Phys.* **2000**, *112*, 4090.

(6) Hold, U.; Lenzer, T.; Luther, K.; Symonds, A. C. *J. Chem. Phys.* **2003**, *119*, 11192.

(7) Nilsson, D.; Nordholm, S. *J. Chem. Phys.* **2002**, *116*, 7040.

(8) Nilsson, D.; Nordholm, S. *J. Chem. Phys.* **2003**, *119*, 11212.

(9) Lenzer, T.; Luther, K.; Nilsson, D.; Nordholm, S. *J. Phys. Chem. B* **2005**, *109*, 8325.

(10) Reichardt, C. *Diploma Thesis*, University of Göttingen, 2004.

(11) Frerichs, H.; Lenzer, T.; Luther, K.; Reichardt, C.; Schwarzer, D. To be published.

(12) Petek, H.; Fujiwara, Y.; Kim, D.; Yoshihara, K. *J. Phys. Chem.* **1988**, *110*, 6269.

(13) Fuss, W.; Kosmidis, C.; Schmid, W. E.; Trushin, S. A. *Chem. Phys. Lett.* **2004**, *385*, 423.

(14) Nikowa, L.; Schwarzer, D.; Troe, J. *Chem. Phys. Lett.* **1995**, *233*, 303.

(15) Champagne, B. B.; Pfanstiel, J. F.; Plusquellic, D. F.; Pratt, D. W.; van Herpen, W. M.; Meerts, W. L. *J. Phys. Chem.* **1990**, *94*, 6.

(16) Takahashi, M.; Kimura, K. *J. Phys. Chem.* **1995**, *99*, 1628.

(17) Brey, L. A.; Schuster, G. B.; Drickamer, H. G. *J. Am. Chem. Soc.* **1979**, *101*, 129.

(18) Waldeck, D. H. *Chem. Rev.* **1991**, *91*, 415.

(19) Schroeder, J.; Steinel, T.; Troe, J. *J. Phys. Chem. A* **2002**, *106*, 5510.

(20) Chiang, W.-Y.; Laane, J. *J. Chem. Phys.* **1994**, *100*, 8755.

(21) Courtney, S. H.; Balk, M. W.; Philips, L. A.; Webb, S. P.; Yang, D.; Levy, D. H.; Fleming, G. R. *J. Chem. Phys.* **1988**, *89*, 6697.

(22) Felker, P. M.; Zewail, A. H. *J. Phys. Chem.* **1985**, *89*, 5402.

(23) Syage, J. A.; Felker, P. M.; Zewail, A. H. *J. Chem. Phys.* **1984**, *81*, 4706.

(24) Greene, B. I.; Hochstrasser, R. M.; Weisman, R. B. *J. Chem. Phys.* **1979**, *71*, 544.

(25) Greene, B. I.; Hochstrasser, R. M.; Weisman, R. B. *Chem. Phys.* **1980**, *48*, 289.

(26) Perry, J. W.; Scherer, N. F.; Zewail, A. H. *Chem. Phys. Lett.* **1983**, *103*, 1.

(27) Majors, T. J.; Even, U.; Jortner, J. *J. Chem. Phys.* **1984**, *81*, 2330.

(28) Amirav, A.; Jortner, J. *Chem. Phys. Lett.* **1983**, *95*, 295.

(29) Baskin, J. S.; Banares, L.; Pedersen, S.; Zewail, A. H. *J. Phys. Chem.* **1996**, *100*, 11920.

(30) Lienau, C. Ph.D. Thesis, University of Göttingen, 1991.

(31) Leitner, D. M.; Levine, B.; Quenneville, J.; Martinez, T. J.; Wolynes, P. G. *J. Phys. Chem. A* **2003**, *107*, 10706.

(32) Beyer, T.; Swinehart, D. F. *Comm. Assoc. Comput. Machines* **1973**, *16*, 379.

(33) Schroeder, J.; Steinel, T.; Troe, J. Unpublished results.

(34) Tee, L. S.; Gotoh, S.; Stewart, W. E. *Ind. Eng. Chem. Fundam.* **1966**, *5*, 356.

(35) Edminster, W. *Pet. Refiner.* **1958**, *37*, 173.

(36) *Handbook of Chemistry and Physics*, 77th ed.; CRC Press: Boca Raton, FL, 1996.

(37) Reid, R.; Prausnitz, J.; Poling, B. *The Properties of Gases and Liquids*, 4th ed.; McGraw-Hill: New York, 1977.

(38) Landau, L. D.; Teller, E. A. *Phys. Z. Sowjetunion* **1936**, *10*, 34.

(39) Lenzer, T.; Luther, K.; Troe, J.; Gilbert, R. G.; Lim, K. F. *J. Chem. Phys.* **1995**, *103*, 626.

(40) Clary, D. C.; Gilbert, R. G.; Bernshtein, V.; Oref, I. *Faraday Discuss.* **1995**, *102*, 423.

(41) Lendvay, G. *J. Phys. Chem. A* **1997**, *101*, 9217.